

Multi-Sensor Integrated Sensing and Communication for Critical Infrastructure Protection

Reiner Thomä*¹, Gerd Sommerkorn*¹, Christian Schneider*[†], Thomas Dallmann*[†]

*Technische Universität Ilmenau, Institute for Information Technology, Ilmenau, Germany

[†]Fraunhofer Institute of Integrated Circuits, Dep. EMS, Ilmenau, Germany

Abstract—Integrated Sensing and Communications (ISAC) will become a service in future mobile communication networks. It enables the detection and recognition of passive objects and environments using radar-like sensing. One promising first application is the protection of critical infrastructure (CI), for example by monitoring the lower airspace above sensitive sites or facilities to prevent unauthorized drone overflights. Our proposal is based on the concept of a distributed multi-sensor (MS)-ISAC. We assume deploying three or more additional passive sniffing sensors near the protected site (PS) of a CI. The sniffers are connected via Downlink (DL) / Uplink (UL) to the distant illumination base station (BS). Multistatic range-Doppler estimation, including synchronization, is performed according to the Cooperative Passive Coherent Location (CPCL) principle. The multistatic architecture has several advantages over the often considered quasi-monostatic architecture where one sniffer is located close to the base station. We discuss the advantages and disadvantages of both approaches and compare their performance for the considered use case in terms of coverage and geometric dilution of precision (GDoP).

I. INTRODUCTION AND MOTIVATION

The use of unmanned aerial vehicle (UAV), also known as drones, is becoming increasingly popular not only among hobbyists but also for commercial applications in civil engineering, agriculture and forestry, logistics, search and rescue, etc. Mobile Network Operators (MNOs) are preparing to support uncrewed aircraft systems traffic management (UTM) within the U-Space framework, the lower airspace designated and regulated for UAVs. Similar to manned civil aviation, ensuring the safety of air traffic in U-Space requires an independent monitoring system that detects flying objects that, for various reasons, do not comply with applicable regulations. Regardless of this, a potential threat has recently emerged that involves deliberate, unauthorized drone overflights. It can be assumed that these drone activities may be intended for provocation, espionage or even sabotage. Properties that are part of CI are particularly vulnerable to this. In addition to large industrial grounds, logistics centers, and national defense sites, energy, communications, and transportation infrastructure facilities are particularly at risk, as they are often relatively unprotected and distributed across a wide rural area. This results in a latent threat scenario that conflicts with the need for regulated and safe commercial use of U-Space. While remote-controlled drones can be easily detected via radio surveillance due to their radio emissions, malicious drones conceal their presence by not transmitting any active signals. Passive drones can only be

detected by radar systems when the target area is illuminated by a radio transmitter.

However, area-wide radar monitoring of U-space is not viable by existing governmental air-traffic control because of several reasons, including limited radar coverage, regulatory issues, technical, and economic effort. What we need is a ubiquitous, scalable, and cost-effective sensor system for monitoring the lower airspace that aggregates a nationwide situational picture. It should enable the integration of additional sensors and external information, generate a situation report as needed, and make this report available to the relevant security authorities and operators of critical infrastructure for decision-making purposes. The challenges are manifold. For instance, there are not enough radio frequency bands available for dedicated radar sensors. In contrast, the seamless integration of radar sensing into existing mobile networks promises a sustainable solution that conserves resources by reusing existing infrastructure and allocated frequency bands. This is known as ISAC. In addition to a comprehensive radio interface for sensing, ISAC provides the entire network infrastructure which is used for sensor control, data transport and fusion including edge processing. The actual local ISAC data can be linked with data from other sensors and fused between sensor clusters. The MNO takes responsibility for administering the ISAC sensing quality on the cluster or network level (“Sensing as a Service”). This service is made available to various users. Eventually a comprehensive situational picture is aggregated. To this end, the compressed information from various local ISAC clusters of different operators is aggregated, and, where applicable, combined with information from other sources. The service at this level is tailored to the requirements of the respective client.

Even though ISAC may have many facets and standardization is still underway (3GPP, ETSI), in this article, we will propose a pragmatic approach that enables ISACs for the use case of CI protection briefly described above; see also [1]. Our proposal relies exclusively on existing 4G/5G radio signaling schemes and avoids making any changes to the hardware of the BSs or to their internal radio access network (RAN) protocols. We recommend installing three or more additional sniffing sensors near the PS. These sniffers act as distributed MS-ISAC [2] sensors and are connected to the BS as standard user equipment (UE) devices. This is basically different from other proposals (e.g. [3]) where a sniffer is deployed close to the BS to mimic a monostatic radar. We will demonstrate that our

setup has fundamental advantages in terms of coverage and overall performance.

II. PROPOSED MS ISAC ARCHITECTURE SETUP

Obviously, the current discussion at 3GPP about ISAC architectures still seems to focus on the monostatic case for infrastructure centric ISAC [4]. As true full duplex radio access is not in reach, quasi-monostatic access is considered, where an auxiliary sniffer device close to the BS is used [3]. Apart from the strong direct feed trough (self-interference), there are several drawbacks of this setup. The first problem concerns target localization estimation, which, in the case of a single station (SS)-ISAC, with co-located transmit and receive antennas, requires not only range estimate (distance to gNB) but also an estimate of the direction of arrival. However, common gNB array access and signal processing is not very well suited for direction of arrival (DoA) estimation. It is more suitable for beamforming (spatial precoding), which allows only low resolution DoA estimation, e.g. 12.7° to ca. 25° beamwidth at the sector corners (because of beam squint) for an 8 element uniform rectangular array (URA) in azimuth. Consequently, the cross-range resolution and accuracy decreases as the distance from the target increases. That does not rule out the possibility of greater DoA estimation accuracy in a high signal-to-noise ratio (SNR) regime with proper off-grid beampattern interpolation. But because of the radar equation, SNR decreases with R^{-4} , where R is the radial distance to the target. Therefore, monostatic SS-ISAC has often an unsatisfactory geolocation performance. [3] does not even discuss DoA estimation, but only range-Doppler estimation, which may be sufficient for target detection in SS-ISAC, but not for target localization.

True multi-target high resolution DoA estimation is possible only with mutual antenna correlation matrix subspace processing (Estimation of Signal Parameters via Rotational Invariance Techniques (ESPRIT), Multiple Signal Classification (MUSIC)) or with model-based maximum likelihood methods. Both are not directly compatible with standard spatial precoding processing (see [2] for high resolution DoA estimation with

spatial precoding). Therefore, often only beam-specific range-Doppler estimation is considered [5]. Another limitation is that a monostatic single station radar can only estimate the radial speed of the target since there is no cross-range Doppler shift measurement available. This is because of a lack of geometric degrees of freedom. Moreover, a monostatic radar cannot deliver any diversity gain for more reliable detection (see the "stealth" problem). Multiple monostatic sensing could help a bit. However, the cellular network is not designed for overlapping radio access. Therefore, it is highly unlikely that a target would be visible at the same time from multiple macro BSs belonging to the same MNO, perhaps except from target locations at the cell borders. However, these cases are rare as resources of neighboring gNBs are allocated towards mutual interference mitigation.

Distributed MS-ISAC potentially avoids all the disadvantages mentioned above for SS-ISAC. The design principles and advantages of MS-ISAC were comprehensively worked out in [2]. According to the prospective use case of critical infrastructure protection, we will focus on infrastructure centric ISAC. This means that only the RAN infrastructure and some dedicated auxiliary UE equipment that is registered and qualified for the this specific sensing service is involved in the sensing cycle. Third party communication UEs are not directly included, except that the communication DL to some contractual user is reused (required) for scene illumination.

There are several approaches for distributed MS-ISAC. Here we assume multiple sniffers acting as remote (hence bistatic) sensors. These sniffers are deployed as dedicated devices at strategically selected locations on behalf of the mobile network operator. They are connected as normal UEs to the gNB via UL and DL, see Fig. 1. We refer to this approach as multi-sensor using user equipment (MS_{UE})-ISAC. The UL / DL connection already ensures receiver (Rx)-transmitter (Tx) frame synchronization. The UE sniffers receive the DL and perform sensing in the MS_{UE}-ISAC broadcast mode using the full multiuser physical downlink shared channel (PDSCH) data stream together with all reference signals transmitted in DL. This means that all 5G New Radio (NR) signaling, scheduling, and precoding functions intended for communication can also be used for ISAC, e.g. to use reference and pilot signals for sensing channel state estimation, equalization and link adaptation. The idea behind is the CPCL principle, also known as cooperative passive radar described at first in [6]. With CPCL we can make sure that the full PDSCH communication data stream is used for bistatic delay-Doppler estimation at the Rx. This explains why the frequency resources allocated for communication are reused entirely for radar sensing, thereby maximizing the SNR compared to ISAC approaches that use only reference and pilot signals. Also, position reference signals (PRSs) can be activated in DL if there is not enough communication capacity requested. This even works in the multiuser downlink, since like in passive radar the sensor does not distinguish with respect to the dedicated receiver. Only the transmitted waveform, not the authorized data content, must be recovered at the UE to be used as correlation reference to

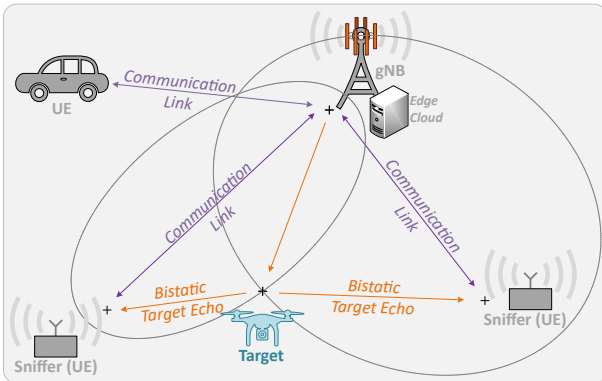


Fig. 1: Generic MS-ISAC architecture. The two sniffers are connected to the next generation Node B (gNB) by the regular UL / DL. The estimated excess time of flight (eToF) are indicated as ellipses. The crossing point is the target position.

calculate eToF and excess Doppler (eDoppler). First single link target related location parameters are calculated at the UE and transmitted via the UL for fusion of data collected from all sniffers at the gNB on the application level. Local estimation at the UE is import for data reduction. The procedures must consider that joint target detection, multitarget data association and 3D estimation of the dynamic target state vector in the fusion center at the gNB becomes possible.

Key advantages of MS-ISAC over the (quasi) monostatic SS-ISAC are: (i) A full 3D dynamic target state estimation is possible through multilateration (bistatic distance and Doppler) and thus without DoA estimation; (ii) A suitable distribution of sniffer positions around the target area not only enables 3D multilateration but also significantly improves the radar link budget. This is particularly true when the area to be observed is clearly defined and not too large, and when the illuminating macro gNB is not too close. This is a situation which is very typical for critical infrastructure protection in rural areas. An excess number of sniffers allows further reduction of estimation variance and can detect outliers the may happen if the line of sight to the target is coincidentally obstructed; (iii) In the specific geographical situation described, it is probable that the dedicated UE sniffer devices are served by the same DL transmission beam, and this beam also illuminates the targets. Therefore, we don't need target specific spatial precoding since the regular precoding requested by the sniffer UE is sufficient.

Another key advantage of the CPCL principle is that excess time of arrival (eToA) and eDoppler measurements reduce to differential coherent methods since excess target range and Doppler are measured relative to direct Tx to Rx line of sight (LOS) from the same impulse response. This largely relaxes transmit-receive synchronization [2]. EToA and eDoppler measurements are based on correlation, which requires knowledge of the transmitted waveform used as correlation reference at the receiver. Although standard orthogonal frequency-division multiplexing (OFDM) equalization already provides an initial estimate of the transmitted waveform, the result is not sufficient for ISAC. Reasons are twofold: The dynamic range requirements for ISAC are generally higher than those for communication. The error is due to noise and poor interpolation from sparse channel state information (CSI) estimates. Another reason may be nonlinear distortion at the power amplifier which is not equalized. To enhance the quality of correlation reference recovery, we proposed a concatenated two step retrieval procedure (turbo CPCL, [2]) that starts with standard CSI based equalization for first transmit signal recovery and continues with a second step that uses the complete PDSCH communication data estimated in the first step. This extended equalization is also necessary because the MS-ISAC broadcast mode requires equalization of the entire multiuser downlink which is not equalized in a standard communication receiver.

III. REALISTIC DEPLOYMENT EXAMPLE

We have chosen a realistic example scenario as given in Fig. 2. The PS is a solar field, indicated by the blue dashed

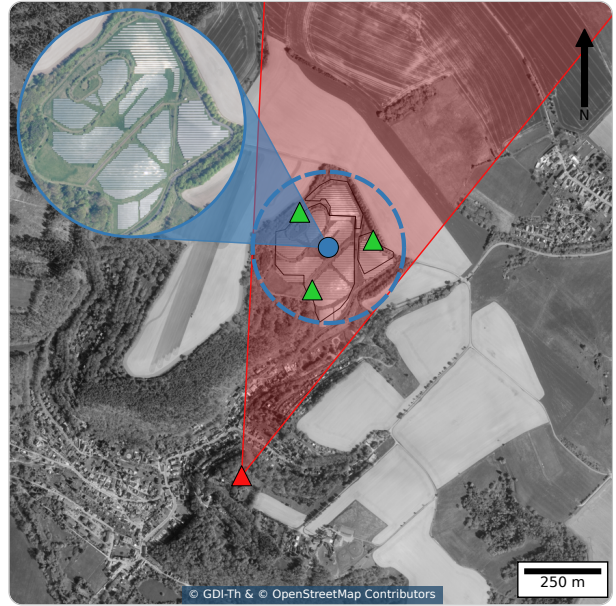


Fig. 2: Example deployment scenario consisting of a solar field that represents the PS and a remote macro BS at an elevated position on a hill near Bad Salzungen, Germany. The three hypothetical sniffer UEs are indicated as green triangles, the BS is the red triangle.

circle, with an approximate diameter of 500 m. We assume three sniffer UEs located at the perimeter of the solar field. The elevated BS is ≈ 800 m away (relative to the median of the sniffers positions).

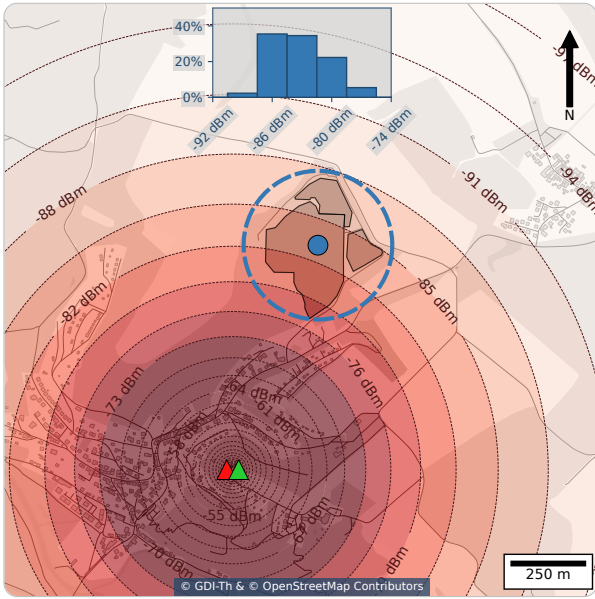
The BS antenna and the solar array are located at roughly the same height. With the regular elevation beamwidth, it should be no problem to illuminate the lower airspace over the specified distance. Fig. 2 also shows the 3 dB azimuth contour of the DL transmission beam that is requested by the three UE sniffers. It appears that the target is also illuminated by the same beam. Since the BS's coverage area extends beyond the target area, there may be further communication users located behind the solar array hosted by the same beam who request DL data traffic which helps to better illuminate the target.

IV. MS ISAC COVERAGE ANALYSIS

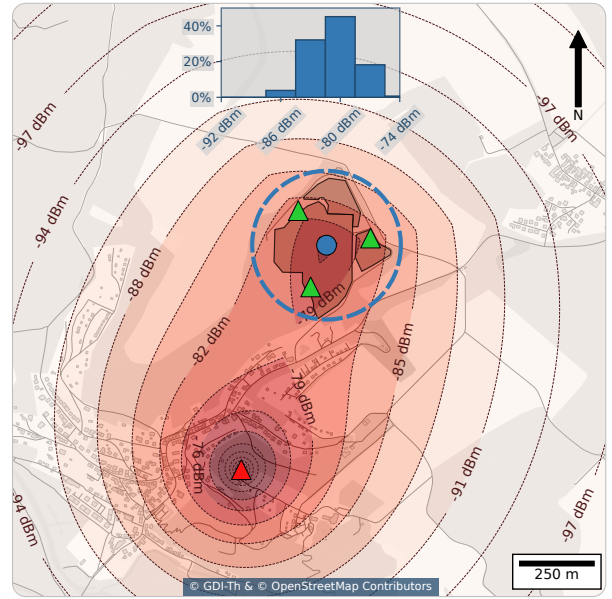
Radar system performance depends on the received power P_r reflected from the target s as given in the logarithmic form for the general bistatic configuration:

$$P_r = P_t + G_t + G_r + \sigma_s + 20 \log_{10}(\lambda) - 30 \log_{10}(4\pi) - 20 \log_{10}(R_{t \rightarrow s}) - 20 \log_{10}(R_{s \rightarrow r}). \quad (1)$$

where P_t is the transmitted power (in dBm), G_t and G_r are the transmitter and receiver antenna gains (in dBi), λ is the wavelength (in m), $R_{t \rightarrow s}$ and $R_{s \rightarrow r}$ and are the transmitter-to-target and target-to-receiver distances (in m), respectively. σ_s denotes the bistatic Radar Cross Section (RCS) that describes the fraction of power scattered from the target to the receiver within one resolved range bin. Here it is given in dBsm. The RCS must be regarded as a random variable whose expected



a) Monostatic case



b) Multistatic case

Fig. 3: Spatial distribution of the simulated received power P_r within the deployment scenario (represented by isolines), with the corresponding power distribution across the PS illustrated as an inset histogram.

value depends on the size, material, and orientation of the target and whose variance is related to the structure of the target. Moreover, it depends on the polarization and angles of the impinging and outgoing waves. Equation (1) considers only propagation in free space routed over the target, without the LOS between the transmitter and the receiver, and without clutter. By introducing the range ratio

$$a = \frac{R_{t \rightarrow s}}{R_{s \rightarrow r}}, \quad (2)$$

the independent distance terms in eq. (1) can be unified.

$$P_r = P_t + G_t + G_r + \sigma_s + 20 \log_{10}(\lambda) - 30 \log_{10}(4\pi) - 40 \log_{10}(R_{t \rightarrow s}) + 20 \log_{10}(a). \quad (3)$$

We distinguish the following cases for the range ratio a :

$$a = \begin{cases} > 1 & R_{t \rightarrow s} > R_{s \rightarrow r} \\ = 1 & R_{t \rightarrow s} = R_{s \rightarrow r} \text{ (monostatic case).} \\ < 1 & R_{t \rightarrow s} < R_{s \rightarrow r} \end{cases} \quad (4)$$

For our deployment scenario in section III we now compare a monostatic and a multistatic radar configuration side by side assuming the following basic system parameters:

TABLE I: System simulation parameters.

Parameter	Monostatic	Multistatic
P_t	44 dBm	
G_t	16 dBi	
G_r	16 dBi	10 dBi
σ_s	-10 dBsm	
λ	0.4283 m / @700 MHz	

The simulation results for both setups are illustrated in Fig. 3. While the monostatic power follows eq. (1), the multistatic

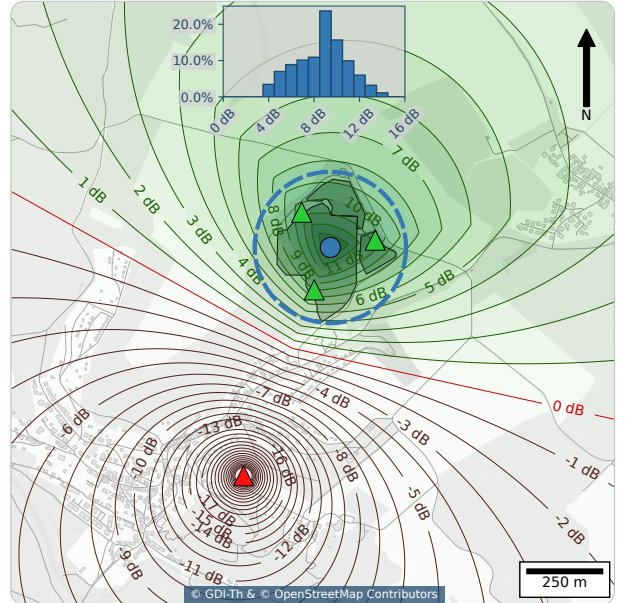


Fig. 4: Spatial distribution of the range ratio a within the deployment scenario (represented by isolines), with the corresponding distribution across the PS illustrated as an inset histogram.

scenario evaluates three separate bistatic configurations, combining them into a joint dataset based on a worst-case selection of the weakest power level.

It can be seen clearly that the received power within the area to be protected is consistently higher for the multistatic configuration. This effect is driven by the shorter receiver ranges $R_{s \rightarrow r}$ compared to the monostatic baseline.

In terms of the previously introduced range ratio given in eq. (2), this geometric advantage corresponds to an increased

value of $a > 1$, which scale-up the received power via the $+20 \log_{10}(a)$ term in eq. (3). Fig. 4 illustrates the spatial distribution of the range ratio a . Following the worst-case approach, the three separate bistatic configurations are combined into a joint dataset based on the minimum power level selection. The distribution of the range ratio a illustrated in Fig. 4 is a direct function of the distance between the illuminating BS and the deployment's PS. A comparison with Fig. 5 highlights this trend, showing that the bistatic gain intensifies as the hypothetical distances increase.

While eq. (3) describes the received power resulting from propagation in free space, the radar performance further depends on the receiver's noise figure, the correlation matched filter correlation gain, and the coherent integration time. The resulting SNR determines not only the target detection probability. It also determines the variance of the bistatic range estimate $\hat{\tau}$ according to the Cramér-Rao lower bound (CRLB) with OFDM bandwidth B

$$\text{var}(\hat{\tau}) \geq \frac{3}{2\pi^2 B^2 \text{SNR}} \quad (5)$$

From the measured bistatic eToF and eDoppler values the 3D dynamic state vector in Euclidean coordinates is calculated as described in [2]. The resulting variance of position and speed scales with a number that depends on the spatial distribution of the sniffers according to an error propagation mechanism known from satellite navigation as GDoP [7]. Fig. 6 shows the rms scaling reduced to the two horizontal dimensions x, y as an example. The rms scaling factor is therefore called horizontal dilution of precision (HDoP) with position estimate \hat{x}, \hat{y} :

$$\text{HDoP} = \sqrt{\text{var}(\hat{x}) + \text{var}(\hat{y})}. \quad (6)$$

V. RESULTS AND DISCUSSION

The distributed MS_{UE}-ISAC approach which uses dedicated sniffers units deployed close to the target area promises a high SNR gain compared to the common (quasi) monostatic setup especially when the area to be protected is well defined, finite, and in some distance to the illuminating gNB. The reason for this is that the bistatic radar equation then reduces to the

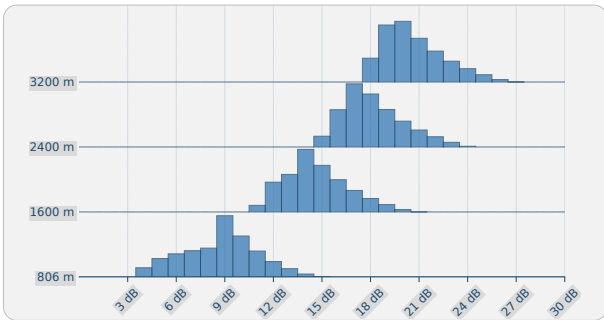


Fig. 5: Range ratio distributions across the PS illustrated as histograms depended on the distance of the BS (806 m corresponds to *real* distance in the deployment scenario, see Fig. 4).

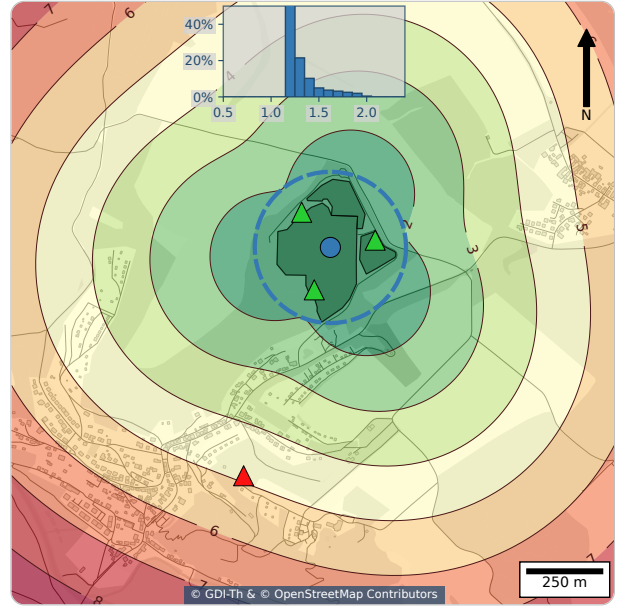


Fig. 6: HDOP within the deployment scenario (represented by isolines), with the corresponding distribution across the PS illustrated as an inset histogram.

case where only the Tx to target path dominates the end-to-end attenuation and the other path contributes less. Another advantage is that the direct feed-through from the transmitter to the receiver is drastically reduced. While strong Tx to Rx interference is often complained about in the quasi-monostatic SS-ISAC approach since it may saturate the receiver, the direct link in the distributed bistatic case is important, since it serves as a reference for differential time of flight (ToF) and Doppler measurement, thereby reducing synchronization issues a lot. Therefore, the sniffers should be placed to have LOS to the gNB. The spatial distribution of the sensors (typically three or more) around the target area allows for the acquisition of a sufficient number of geometric degrees of freedom to enable the estimation of the complete 3D dynamic target state vector (position and speed) by multilateration. Finally, we would like to point out that the SNR improvement we achieve by properly positioning the sniffer UEs not only extends the detection range. Perhaps even more importantly, we can reduce the estimation variance within a given target distance according to the CRLB, eq. (5), which improves localization accuracy. The SNR influence to CRLB also explains that lower operating frequencies (e.g. frequency range 1 (FR1) low- and midband) with their lower bandwidths are not as disadvantageous as often presumed since that is partly compensated by higher SNR (for a given distance). In addition, the lower antenna directivity comes as an advantage because target beam search is relaxed.

As for the limited target resolution relative to the direct LOS link between the Tx and Rx, as well as with respect to the resolution of multiple targets, we suggest that resolution is achieved not only in the distance dimension but also in the Doppler dimension. And since the LOS response is well known (actually we have estimated the correlation reference),

we can remove this contribution even if it overlaps to the target response by some kind of interference cancellation procedure as long as the receiver is in its linear operation mode. See [2] for some deeper discussion of model based high resolution in joint range and Doppler dimension.

Finally, we must point out that the performance evaluation of our proposal for a distributed MS_{UE} -ISAC presented in this article is conducted solely on a relative basis, which consists in comparison to the (quasi) monostatic case. If we assume that the same gNB parameters (frequency, bandwidth, equivalent isotropically radiated power (EIRP)) are applied in both cases and if the receiver achieves the same matched filter processing gain and the same coherent radar integration time, the SNR gain indicated by the range ratio a in eq. (3) and Fig. 4 and 5 results only from the choice of the positions of the sniffer UEs. Some difference still may remain due to the size of the antenna arrays on the sniffers in both cases. The antenna array of a sniffer located near the gNB may have higher gain than that of the sniffer located near the target, since the latter requires full 360° coverage. On the other hand, since we have three or more sniffers around, we can achieve another least-mean-squares (LMS) estimation gain by fusing the measurement from those sniffers.

VI. OUTLOOK AND CONCLUSION

We have proposed a distributed MS-ISAC architecture consisting of multiple dedicated sniffer units connected to the base station via the standard multiuser DLs / ULs. The advantages include extended coverage and low GDoP value within the give service area. Another asset is that the BS's RAN interface would not require any significant changes to the hardware or software, which could lower the barriers to acceptance for mobile network operators. The sniffer works similarly to the well-known passive radar. But according to CPCL, it can interact with the base station at the application software level.

We have shown that, provided a suitable geometric arrangement of the sniffers is possible, the MS_{UE} -ISAC approach outperforms the conventional (quasi-)monostatic approach in several respects. However, one might argue that the coverage area is possibly too limited and that the concept of using dedicated sniffers is not a suitable approach for achieving comprehensive wide area coverage. As a solution to this dilemma, we propose rethinking the well-known concept of "umbrella cells" and adapting it to ISAC. If a macro cell - especially in the lower FR1 band - covers a large area, there will usually be several small-cell base stations from the same operator within reach. In that case, the respective mobile network operator can reuse its own sites to host dedicated sniffer units, which requires installing an additional FR1 receiving antenna and the corresponding sniffer receiver. This configuration works the same way as the MS_{UE} -ISAC sniffer, except that it does not need a full UL / DL for data reporting since we have the network backbone at hand which would be enough for compressed data reporting. Wide area coverage is supported by the wider service range at lower

FR1 frequencies while higher resolution may be achieved at local sensing hot spots with the MS_{UE} -ISAC approach at FR1 midband or prospective frequency range 3 (FR3) frequencies. This creates a comprehensive, hierarchically structured UE monitoring network that can be gradually put into operation and expanded.

An even more general and powerful architecture for infrastructure-oriented MS-ISACs can be achieved when a Cooperative Multi-Point (CoMP) RAN network is available to serve as a MS ISAC cluster, for example, within a campus network that covers a large industrial area requiring protection. In this case, we have several radio units (RUs) connected to a distributed unit (DU) and the collocated baseband unit (BBU) pool by a fiber-optic fronthaul link while the functional split follows the open radio access network (O-RAN) convention. We refer to this approach as multi-sensor using radio unit (MS_{RU})-ISAC. This architecture approach allows fast resource allocation and RUs access coordination. It enables a full meshed MS-Multiple Input Multiple Output (MIMO) architecture as each RU can act as an illuminator while all others serve as sensors [2].

Acknowledgments

This work is partially supported by the the Federal Ministry of Research, Technology and Space of Germany (BMFTR) in the projects SENSATION (grant number: 16KIS2531) and Open6GHub+ (grant number: 16KIS2406) as well as by the Deutsche Forschungsgemeinschaft (DFG) under the project JCRS CoMP (grant number: TH 494/35-1).

REFERENCES

- [1] Victor Shatov et al. "Joint Radar and Communications: Architectures, Use Cases, Aspects of Radio Access, Signal Processing, and Hardware". In: *IEEE Access* 12 (2024), pp. 47888–47914. DOI: 10.1109/ACCESS.2024.3383771.
- [2] Reiner S. Thomä et al. "Distributed Multisensor ISAC". In: *npj Wireless Technology* 2.1 (2026). DOI: 10.1038/s44459-026-00041-2.
- [3] Stefan Saur et al. "Reliable UAV Detection with ISAC". In: *arXiv preprint arXiv:2605.23561* (2026). DOI: 10.48550/arXiv.2605.23561.
- [4] Steve Blandino et al. *Evaluation of gNB Monostatic Sensing for UAV Use Case*. 2026. arXiv: 2604.02205 [eess.SP].
- [5] Musa Furkan Keskin et al. "Fundamental Trade-Offs in Monostatic ISAC: A Holistic Investigation Toward 6G". In: *IEEE Transactions on Wireless Communications* 24.9 (2025), pp. 7856–7873. DOI: 10.1109/TWC.2025.3563197.
- [6] Reiner S. Thomä et al. "Cooperative Passive Coherent Location: A Promising 5G Service to Support Road Safety". In: *IEEE Communications Magazine* 57.9 (Sept. 2019), pp. 86–92. DOI: 10.1109/MCOM.001.1800242.
- [7] Richard B. Langley. "Dilution of Precision". In: *GPS World* 10.5 (May 1999), pp. 52–59.